Applied Catalysis B: Environmental 142–143 (2013) 387–395

Contents lists available at SciVerse ScienceDirect

Applied Catalysis B: Environmental

journal homepage: www.elsevier.com/locate/apcatb

Gas phase acetone self-condensation over unsupported and supported Mg–Zr mixed-oxides catalysts

Laura Faba, Eva Díaz, Salvador Ordóñez*

Department of Chemical Engineering and Environmental Technology, University of Oviedo (Faculty of Chemistry), Julián Clavería s/n, 33006 Oviedo, Spain

ARTICLE INFO

Article history:
Received 2 April 2013
Received in revised form 13 May 2013
Accepted 22 May 2013
Available online 28 May 2013

Keywords:
Biomass upgrading
Aldol-condensation
High surface area graphites
Carbon nanofibers
Base catalysis

ABSTRACT

Acetone gas phase aldol condensation over bulk and carbon-supported Mg–Zr has been studied in this work. The condensation yields C6 (mainly mesityl oxide) and C9 (phorones, isophorones and mesitylene) compounds, depending on reaction temperature and distribution of acid and basic sites. The influence of the temperature (323–723 K) was studied, higher C9 selectivities being obtained at higher temperatures (close to 50%). The influence of the concentration and the distribution of basic and acid sites was analyzed by comparing the results obtained with the bulk Mg–Zr and with Mg–Zr supported on non-microporous carbonaceous materials: high surface area graphites (HSAG) and carbon nanofibers (CNF). In addition, two different preparation methods (dry impregnation and co-precipitation) were tested.

The performance of the catalysts is related to the distribution of acid and basic sites. Acid–basic pairs are needed for the acetone condensation, weak acidity for dehydration and cyclation reactions, and the strongest basicity for the condensation of mesityl oxide.

1. Introduction

Although most of the acetone is nowadays produced from petrochemical feedstock by the cumene process [1], emerging technologies based on the chemical or biological biomass processing will become the acetone into an interesting bio-based platform molecule. Therefore, ABE fermentation allows the simultaneous production of butanol, ethanol and acetone from agricultural wastes [2], whereas biomass pyrolysis can also yield significant amounts of acetone [3]. The upgrading of this acetone (up to now mainly used as industrial solvent) is of key interest for process sustainability. Upgrading strategies relies on the formation on new carbon–carbon bonds yielding to more complex molecules, intermediates for many medical, chemical and cosmetic products.

Nowadays, liquid phase aldol condensation is performed for obtaining diacetone alcohol (DAA) and the mesityl oxide (MO), used as precursors of the methyl-isobutyl-ketone (MIBK) [4], an important fine chemical and fuel additive. If this reaction is carried out at higher temperatures and in gas-phase, it can lead to more complex reaction pathways yielding interesting chemicals, such as phorones (linear trimmers), isophorones (cyclic trimmers) or mesitylene [5,6]. Isophorones are important industrial chemicals, having applications in paints, pesticides, adhesives, resins, etc. [7]. Isophorones are industrially obtained by acetone condensation with homogeneous catalysts (KOH) in distillation columns at high temperatures and pressures [8]. The substitution of the homogenous catalysts used in liquid-phase processes by heterogeneous catalysts presents important advantages, as the decrease on the environmental impact of the process and the easiness of catalyst recovery and re-utilization. In addition, the acid–base properties can be tuned in order to increase the selectivity for the desired reaction products. This fact is of key interest in these reactions, since reaction pathways involve acid and basic sites of different strengths [9,10].

The use of MgO or Mg–Al mixed oxides as catalysts for this reaction has been already reported, obtaining promising results [9,11]. Considering that the key reaction (formation of C—C bond by aldol condensation) is catalyzed by medium-strength basic sites, Mg–Zr mixed oxide is suggested as an alternative material to improve the formation of the most valuable isophorones. To the best of our knowledge this catalyst has not been tested in the acetone gas-phase aldol condensation instead of having been obtained good results in similar processes as furfural-acetone aldol condensations [12]. In these materials, bidentate basic sites are associated with medium-strength acid sites which, according to the most accepted mechanism [5], could enhance the cyclation of phorones, yielding higher amounts of isophorones. Besides, the concentration of strong basic sites (considered the main responsible of catalyst deactivation in this kind of reactions) is considerably lower, leading to higher catalyst stability [13].

It was previously observed that the catalytic activity of mixed oxides can be improved by dispersing the active phase onto inert

* Corresponding author. Tel.: +34 985 103 437; fax: +34 985 103 434.
E-mail address: sordonez@uniovi.es (S. Ordóñez).

0926-3373/$ – see front matter © 2013 Elsevier B.V. All rights reserved.
http://dx.doi.org/10.1016/j.apcatb.2013.05.043

Table 1
Morphological and acid–base properties of the catalysts used in this work.

Catalyst	Morphological properties			Active phase dispersion (%)	Basic sites (CO_2-TPD): μmol/g			Acid sites (NH_3-TPD): μmol/g		
	S_{BET} (m^2/g)	D_p (Å)	V_p (cm^3/g)		Bicarbonate	Bidentante	Monodentate	Weak	Medium	Strong
MgZr	78	342	0.8	–	–	120	13	62	239.3	158
MgZr/HSAG100	110	167	0.5	9.2	11	5.5	32	117	–	85
MgZr/HSAG300*	270	83	0.5	–	19	–	19	448	–	–
MgZr/HSAG300	243	80	0.4	10.0	10	17	19	984	–	85
MgZr/HSAG500	337	79	0.6	13.8	10	13	20	489	–	24
MgZr/CNF	41	184	0.2	–	2.1	1.6	38	12	197	114

Source: Adapted from Ref. [15].

supports because the presence of structural defects creates new active sites [14,15]. Inorganic supports generally have distributions of acid/basic sites that interfere on the activity so they were discarded in order to prevent undesired side reactions. On the other hand, carbon nanofibers and high-surface area graphites (HSAG) present good properties for dispersing active phases without altering their chemical behavior [16] and, especially in the case of HSAG, they have unsaturated valences at the edges of the graphitic layers leading the formation of extra anchoring sites for the active phase [17].

The aim of this work is to deeply investigate the mechanism of the gas phase reaction of acetone to its condensation products using unsupported and supported Mg–Zr mixed oxide as catalyst, as well as to determine the main properties needing for improving isophorone selectivity.

2. Experimental

2.1. Catalysts preparation and characterization

Bulk and different carbon-supported magnesia–zirconia mixed oxide were prepared and tested for acetone self-condensation in a fixed bed reactor. The bulk mixed oxide was synthesized using the sol–gel technique firstly described by Aramendía et al. [18].

Graphites and nanofibers were used as supports for the Mg–Zr mixed oxide using two different preparation procedures. High surface area graphites (HSAG100, HSAG300 and HSAG500) were supplied by Timcal S.A. (Switzerland) and the carbon nanofibers (CNF) were supplied by Applied Sciences (Cerdaville, OH). All the supported materials were prepared trying to keep the same Mg/Zr ratio than in the bulk material (Mg/Zr = 4). Mg–Zr/HSAG300* was prepared by the incipient wetness method. In this case, the amount of mixed oxide was limited by the low water solubility of the zirconyl precursor that limited the percentage of the mixed oxide in final catalyst (0.037 g of zirconyl nitrate in 5 g of graphite, leading to Zr concentration of 1 wt%). HSAG100, HSAG300, HSAG500 and CNF were also used as supports using a co-precipitation method, according to the procedure described by Winter et al. [14]. Zirconium content, measured by ICP-MS, of these materials was between 2% (Mg–Zr/HSAG300) and 4% (Mg–Zr/HSAG500), whereas Mg/Zr ratio was kept at 4 for all the HSAG-supported materials. CNF-supported material shows a different behavior with a 5% Zr, but lower Mg/Zr ratio (0.5). In all the cases, the catalysts were treated with a heating rate of 3 K/min to 873 K in a He flow. Further details about the preparation and characterization of these materials are given elsewhere [15].

Morphology and acid–base properties of the resulting catalysts was thoroughly characterized in a previous work [15], being the main results summarized in Table 1. Surface areas obtained were in good agreement with initial areas of the parent supports, whereas mixed oxide dispersion increases as the surface increases. Concerning to the basicity, the overall concentration of basic sites is always lower than for the bulk material, but the concentration of the strongest basic sites (corresponding to monodentate adsorption modes of CO_2) increases in all the cases. Regarding the acidity of the supported catalysts, only weakest sites can be considered because supported catalysts had a desorption peak of NH_3 at temperatures over 800 K, not present in the bulk Mg–Zr material, that was associated with functional groups of the supports [19].

2.2. Reaction system and procedure

The reaction was carried out in a fixed bed reactor consisting of a 0.4 cm i.d. U-shaped quartz placed in a PID-controlled electric furnace. Catalyst samples (150 mg, 50–80 μm particle diameter) was placed over a plug of quartz wool and a thermocouple was placed inside the catalyst bed. The acetone was injected as a liquid in a He flow (0.05 L/min) and vaporized in situ, obtaining a volume concentration of 3.2%. The catalytic particle sizes as well as the initial concentration of acetone in helium were chosen in order to prevent mass transfer effects.

Samples were collected in a cold trap (mixture of liquid nitrogen and isopropanol). They were analyzed by gas chromatography using a Shimadzu GC-2010 equipped with a FID detector and using a 15 m long CP-Sil 5 CB capillary column as stationary phase. Product identification was confirmed by analysis in GC–MS (Shimadzu QP-2010) using the same column and conditions than in the gas chromatograph. Carbon mass balance was checked in all the experiments.

3. Results

3.1. Acetone self-condensation over bulk Mg–Zr oxide

The gas phase condensation of acetone was initially studied using Mg–Zr (bulk) as catalysts. The possibility of diffusional limitations was ruled out based on the Thiele modulus. The low value of Thiele modulus calculated for supported Mg–Zr (4.6×10^{-5}) indicated the absence of diffusion limitations.

The condensation was studied at temperatures between 323 and 723 K. A blank experiment was carried out at the highest temperature using a bed of quartz instead of the catalyst, to confirm that no homogeneous reaction occurs. Overall conversion and selectivity to the main reaction products obtained – diacetone alcohol (C6), mesityl oxide (C6), phorones (C9), isophorones (C9) and mesitylene (C9) – are summarized in Fig. 1. Acetone conversion increases as reaction temperature increases, reaching more than 30% of conversion at 723 K. Reaction patterns are congruent with the results previously reported in the literature with different mixed oxides [9] or other active materials, like TiO_2 [20] or MgO [21]. According to these results, the aldolization of acetone first leads to diacetone alcohol, product than can undergo dehydration into mesityl oxide. Mesityl oxide is the major product detected, mainly at low temperatures, with selectivities higher than 80%. This product is

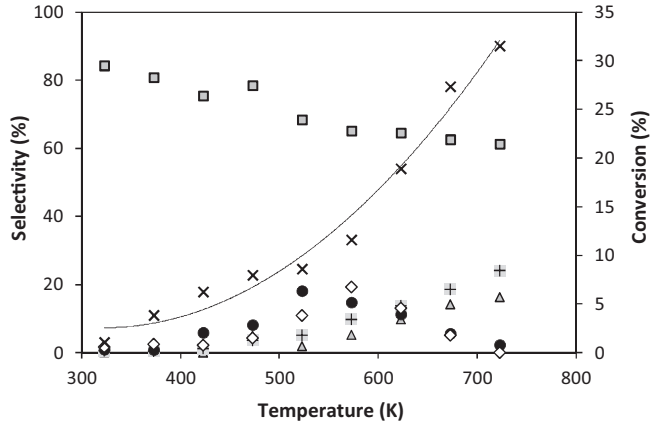

Fig. 1. Influence of the reaction temperature on the conversion (×) and selectivities for the main reaction products in the condensation of acetone over Mg–Zr catalyst: diacetone alcohol (▲), mesityl oxide (■), mesitylene (+), phorones (●) and isophorones (◊).

an α-β-unsaturated carbonyl compound that could react again with acetone leading different linear trimmers, generally called phorones. The selectivity for these compounds increases at high temperatures but never exceeds 20% because they form cyclic compounds: mesitylene and isophorones. The maximum selectivities obtained were 18% for isophorones (at 575 K) and 24% for mesitylene at 723 K. Lumping the different reaction products in terms of their number of carbon atoms, a maximum of 34% of selectivity for C9 fraction was obtained at the most favorable conditions. These values are higher than reported in the literature for other materials tested at the same condition, for example Mg–Al mixed oxides [9]. It is reported that higher temperatures also favors the condensation of two molecules of mesityl oxide yielding non-desired C12 ketones [22]. These products were not detected with this catalyst, being the carbon balance closure higher than 90% at 723 K.

3.2. Acetone self-condensation over carbon-supported Mg–Zr oxide

The effect of supporting the mixed oxide over mesoporous materials was studied considering two different carbonaceous materials: carbon nanofibers (CNF) and high surface graphites (HSAG). Over the last support (HSAG), two different preparation methods were tested, based on impregnation and co-precipitation. Additionally, the reaction was also carried out using the parent CNF and HSAG support as catalysts and the conversions obtained were always lower than 2%, discarding any catalytic effect of the support. Main results, in terms of conversions, C6 selectivity (mesityl oxide and diacetone alcohol) and C9 selectivity (phorones, isophorones and mesitylene) as function of the reaction temperature are summarized in Fig. 2.

Catalyst prepared using the dry-impregnation method (HSAG*) provides the poorest results, maximum conversion being lower than 15% (723 K). By contrast, conversion values of 43 and 54% were obtained at this temperature for CNF and HSAG, respectively. These conversions were, in both cases, higher than the value obtained with the bulk material (32%), in spite of the lower loading of metal oxide.

Concerning to the products distribution, results obtained with nanofibers and graphites followed the same trend observed for Mg–Zr: higher C6 selectivities at low temperatures and higher C9 selectivities at high temperatures. In both cases, it was a significant increase in the C9 selectivities over 500 K. Results by families were not so significant. There was only an increase in the C9 selectivity

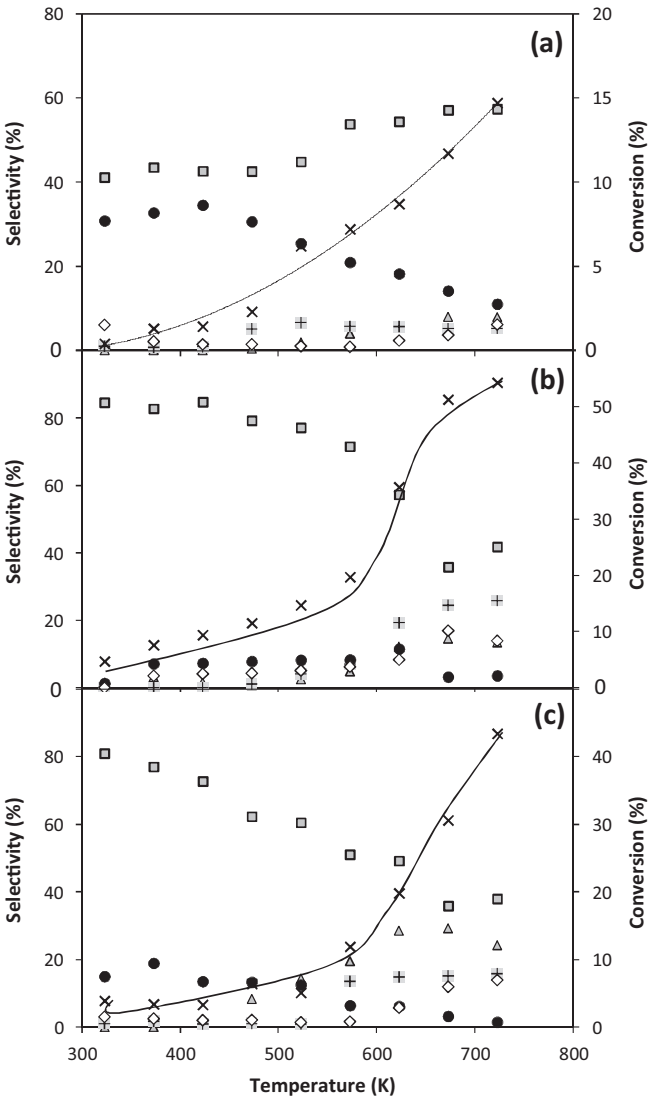

Fig. 2. Influence of the reaction temperature on the conversion and selectivities for the main reaction products in the condensation of acetone over (a) MgZr/HSAG300*, (b) MgZr/HSAG300 and (c) MgZr/CNF (see Fig. 1 for codes).

for the graphite-supported catalysts at temperatures higher than 650 K and the main differenteces were observed in the distribution of each compound.

Concerning to the C6, mesityl oxide is the major compound detected in both cases at all temperatures. This compound is formed by the fast dehydration of diaceton alcohol over acid sites, so the diacetone alcohol (first compound formed) was obtained in much lower concentration, mainly with the nanofibers. At high temperature the mesityl oxide selectivity decreases, in good agreement with the formation of the trimmer compounds.

As to the C9 compounds, phorones were the main adduct detected at low temperatures with both materials. At temperatures below 550 K, HSAG is more active for phorones cycling than CNF, and the selectivities of isophorones and mesitylene are higher with this material. At medium temperatures, the cyclations of phorones were more selective in the case of nanofibers (with almost only mesitylene), whereas there was a balance between mesitylene and isophorones when graphites were used as supports. As well as it occurred with C6 compounds, the differences between both supports were less relevant at the highest temperatures and it reached almost the same selectivity of isophorones. Taking into account that isophorones are considered as the most promising reaction

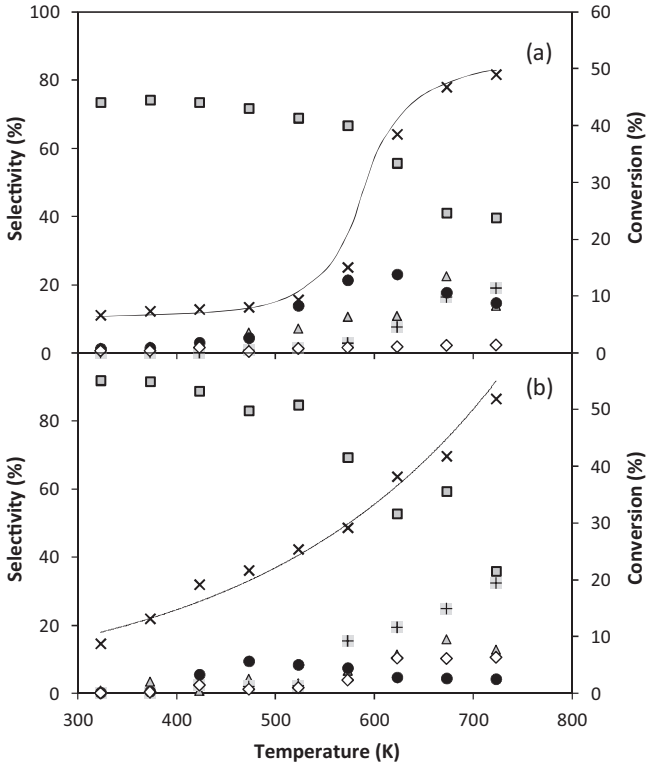

Fig. 3. Influence of the reaction temperature on the conversion and selectivities for the main reaction products in the condensation of acetone over (a) MgZr/HSAG100 and (b) MgZr/HSAG500 (see Fig. 1 for codes).

product, best results were obtained with high surface area graphites (reaching more than 17% isophorones selectivity).

Carbon balances were calculated considering the amount of acetone used as reactant and the concentration of all the compounds detected. These values can be conditioned by the presence of non-desired side reactions and the adsorption of products on the catalytic surface. Three main side reactions have been proposed for this process: the reaction of phorones to form heavy compounds (coke) that can precipitate on the catalytic surface [23], the xylitones formation [22], and the decomposition of mesityl oxide into isobutene and acetic acid [24]. These products were not detected by GC-FID. The carbon balance closure obtained with nanofibers (36% at 723 K) can suggest the presence of important coke deposits over this surface. This effect was not so significant in the case of HSAG (79.8% at 723 K). Therefore, this support was chosen to systematically vary the oxide dispersion for tuning the acid–base properties of the material without modifying the chemistry of the support.

For accomplishing this purpose, two other HSAG with different surface areas were considered (HSAG100, HSAG500). Main activity results are summarized in Fig. 3 in terms of conversions and selectivities. Results are analyzed together with those obtained with MgZr/HSAG300. Regarding acetone conversion, all the graphitic catalysts showed parallel behaviors, reaching, in the three cases, conversions around 50–55% at 723 K (50%, 54.3% and 51.9% with HSAG100, HSAG300 and HSAG500 supports, respectively). These conversions indicate an almost double activity of supported materials in comparison with the bulk material.

Concerning to the C6 compounds, they were the major product at low and medium temperatures, and their selectivities decrease more significantly at temperatures higher than 600 K, especially in the case of MgZr/HSAG500. As to the distribution of the different compounds of each family, same trends were obtained with the three catalysts: the selectivity of mesityl oxide decreases as the temperature increases because it is consumed yielding the trimmers. On the other hand, diacetone alcohol was always a minority compound and never reaches values higher than 12%, although the selectivity to this compound increases as conversion increases. The good correspondence between the results of the three supported materials could be predictable due to the similar distribution of the acid and basic sites.

The second condensation needed to obtain C9 compounds was almost prevented with the HSAG500 support at temperatures under 400 K, whereas more than 14% of C9s were obtained with the MgZr/HSAG300 at the same reaction conditions. Increasing the reaction temperature these differences decreased, in such a way that over 600 K, the highest C9 selectivity was obtained with MgZr/HSAG500, obtaining almost 50%. The distribution of mesitylene, phorones and isophorones (C9 compounds) was clearly conditioned by the reaction temperature: the more noticeable differences were obtained between HSAG100 and HSAG500, whereas HSAG300 has an intermediate behavior more similar to HSAG100 at low temperatures (with almost null production of cyclic compounds) and more similar to HSAG500 at high one (with almost total selectivity of cyclic adducts). It can be concluded that HSAG100 and HSAG300 needed medium temperatures to allow the cyclation of phorones into isophorones, whereas using the HSAG500 the cyclation was promoted at all the temperatures.

Concerning to the carbon balance, a decrease was observed at highest temperatures, mainly in the cases of MgZr/HSAG300 and MgZr/HSAG500: at 723 K, their carbon balances only reach values of 71.8 and 73%, respectively (whereas it was almost 80% with MgZr/HSAG100). This behavior can be justified by the formation of side products (coke and other non-desired products) at high temperatures. According to results obtained and in good agreement with previous works [11], the deactivation is more noticeable at temperatures over 600 K. To check the influence of these side-reactions, the spent catalysts were characterized in order to identify any change in the morphological parameters (physisorption analyses, TEM), quantify possible coke deposits (TPO) or significant modifications in the basicity.

Physisorption analyses (Table 2) showed a general decrease in the surface area, more noticeable in the cases of MgZr/HSAG300 and MgZr/HSAG500 (47.7 and 43.6%, respectively). These results are congruent with the final carbon balance closures. Concerning to the pore volume, there was a light decrease in the three cases, but the effect was less marked than the effect on the surface area. Most of the blocked pores were those with the smallest size, so the general effect is an increase in the pore diameter.

The main reason for the decrease in the surface area is the deposition of carbonaceous deposits over the catalytic surface. This fact was corroborated by TPO analyses of the spent materials. TPO profiles are shown in Fig. 4. In this figure, the decompositions of the original materials are also shown (dashed lines) in order to discriminate between desorption of oxidized carbon deposits and the natural decomposition of the carbon materials at high temperatures in oxidant atmosphere. Concerning to the combustion temperature of the deposits, profiles obtained with MgZr/HSAG100 and MgZr/HSAG300 were very similar and two main peaks can be distinguished, related to two different types of coke deposits. In the case of MgZr/HSAG500, there was a third peak at a temperature higher than the 1100 K, thus there was a different compound deposited on the catalytic surface. Concerning to the amount of coke, the areas obtained were in good agreement with the carbon balance closures; in such a way that higher area was obtained with MgZr/HSAG300.

TEM analyses of the fresh and used catalysts reveal minor increases of catalyst dispersion after the reaction cycle (maximum 5% for the HSAG500 supported catalysts). Therefore, the changes on the acid–base properties of the catalysts upon reaction will cause

Table 2
Morphological and acid–base properties of the spent catalysts.

Catalyst	Morphological properties			Basic sites (CO_2-TPD): μmol/g		
	S_{BET} (m^2/g)	D_p (Å)	V_p (cm^3/g)	Bicarbonate	Bidentante	Monodentate
MgZr/HSAG100	86	175	0.4	13.0	7.8	25.6
MgZr/HSAG300	127	96	0.3	21.9	–	19.7
MgZr/HSAG500	190	94	0.5	0.4	2.9	5.5

the selective blockage of the reactive sites, rather than by changes on the crystallite sizes of the mixed oxide.

In order to study if the basicity (main active parameter) was affected, CO_2-TPD analyses of the spent catalysts were carried out to compare the profiles with those obtained with the fresh materials. Taking into account that these profiles can be conditioned by the desorption of the CO_2 adsorbed over the coke and released during the thermal decomposition of these deposits, TPD of spent catalysts were also done and, in all the cases, the catalysts were pre-treated at 850 K before the CO_2-TPD analyses. The density and the strength of basic sites in spent catalysts (Fig. 5) is summarized in Table 2. There was a general decrease in the strength of the basicity, so the bicarbonate types are less affected by deactivation than bidentate and monodentate sites. The density of basic sites kept almost constant in the cases of MgZr/HSAG100 and MgZr/HSAG300, whereas it decreases close to 80% in the case of MgZr/HSAG500. Analyzing the activity results, at temperatures under 600 K, the best results were obtained with MgZr/HSAG500; however, at higher temperatures, results of MgZr/HSAG300 and MgZr/HSAG500 were similar. These results suggest that, at the highest temperatures, the behavior of MgZr/HSAG500 can be affected by the loss of active sites.

4. Discussion

The evolution of acetone conversion with the temperature was modeled considering first-order kinetic and Arrhenius dependence of kinetic constant with temperature. The goodness of the fit observed in Fig. 6, as well as the unfair fitness obtained considering second order dependence, suggest that the rate controlling step is unimolecular. There is no agreement in the scientific community about the kinetic order of this reaction: several authors consider first order kinetics, being the limiting step the enolate formation [23]; whereas other authors consider a second order kinetics [6]. Among the mechanisms proposed in the literature, first-order kinetics observed in these experiments was in good agreement with those that consider that the controlling step is the formation of a carbanion from the acetone molecule. According to this mechanism, the molecule of acetone interacts with a bidentate

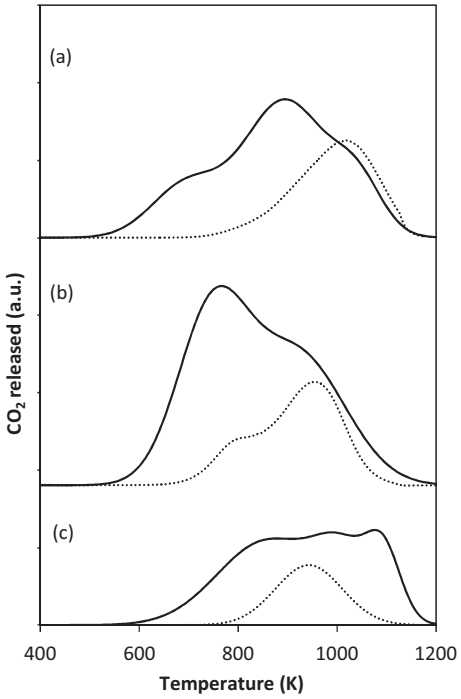

Fig. 4. TPO profiles of the spent catalyst (continuous lines) and the fresh catalysts (broken lines): (a) MgZr/HSAG100, (b) MgZr/HSAG300 and (c) MgZr/HSAG500 catalyst.

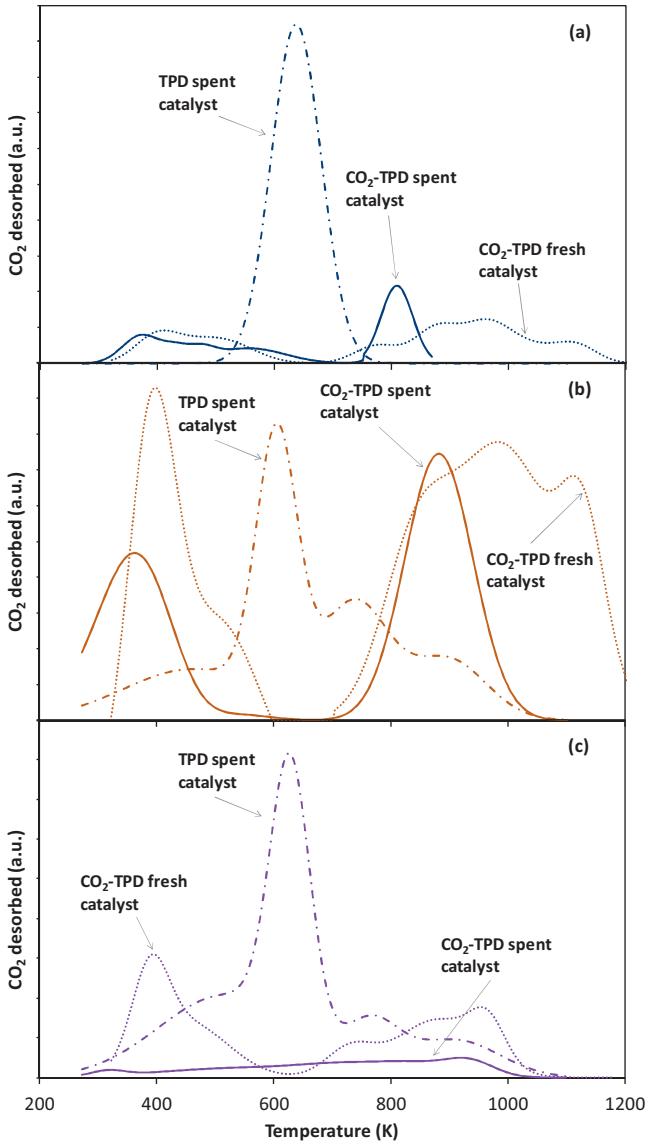

Fig. 5. Comparison between profiles obtained by TPD and CO_2-TPD of spent and fresh catalyst. Results related to (a) MgZr/HSAG100, (b) MgZr/HSAG300 and (c) MgZr/HSAG500 catalysts.

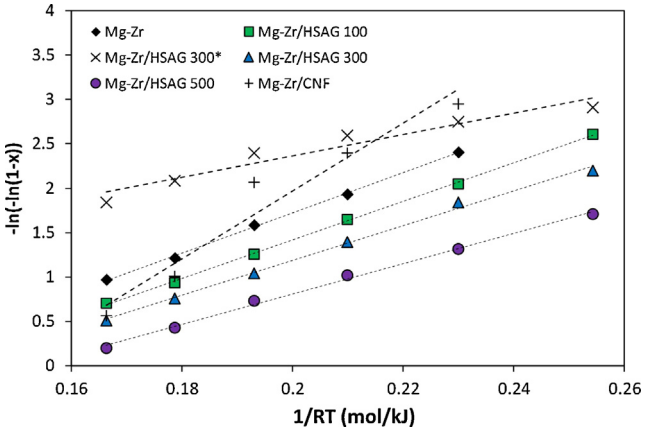

Fig. 6. Arrhenius plot for acetone conversion considering pseudo-first order kinetics for the acetone consumption rate.

basic site of the catalyst and the α-proton is abstracted forming a carbanion. The carbanion attacks the carbonyl group of another acetone molecule yielding primarily diaceton alcohol.

As it can be observed in this figure, graphitic supported bulk mixed oxides and materials synthesized by co-precipitation method show similar trends, whereas the behavior of the Mg–Zr/HSAG300* and the nanofibers were very different. Results show that the activation energy of catalyst supported on high surface area graphites by co-precipitation method were very similar, with an activation energy of 23.5 kJ/mol. Value obtained was congruent with results previously reported in the literature for the self condensation of similar compounds [26,27] and it suggests that the reaction is intrinsically kinetically controlled. This energy decreases to 12 kJ/mol in the case of MgZr/HSAG300*, whereas the value obtained with the MgZr/CNF was sensitively higher (38.2 kJ/mol). These different values justify the special behavior of these two materials and the unusual distribution of the main products. Consequently, these two catalysts will be discarded of the main discussion.

In order to study the influence of the acid/basic sites distribution on the catalyst performance, results obtained with the different supported materials were deeply analyzed. Profiles obtained allow discerning two different situations: reaction at low temperatures (under 550 K, conditions in which the C6 formation is the main process), and reaction at high temperatures (in this case, the acetone condensation leads the C9 formation).

Concerning to the low temperature trends, acetone conversions obtained depend not only on the concentration of basic sites or acid sites independently considered. Mg–Zr/HSAG300 is the catalyst with larger concentration of both kinds of sites but is not the most active catalyst, suggesting that there is an optimal ratio of acid/basic sites, Mg–Zr/HSAG500 being closer to this ideal ratio.

As to the product selectivity, at low temperatures, only the formation of C6 adducts (DAA, MO and IMO) is relevant. The evolution of the selectivity to these compounds with the acetone conversion is depicted in Fig. 7. Although experiments at different temperature cannot be used to quantitative interpretations, plots obtained can be useful for obtaining information about the reaction mechanism. At low temperatures, the C6 selectivities obtained for the supported catalysts (95.9% with MgZr/HSAG500, 87.4% with MgZr/HSAG300 and 81.1% with MgZr/HSAG100) are congruent with the active phase dispersion order: HSAG500 > HSAG300 > HSAG100.

Among these dimmers, the low selectivity for the IMO does not follow any systematic trend, presenting only significant selectivities (but always lower than 9%) only at very low conversions. Concerning to MO, the main product at these conditions, the evolution of the selectivity with the reactant conversion follows the

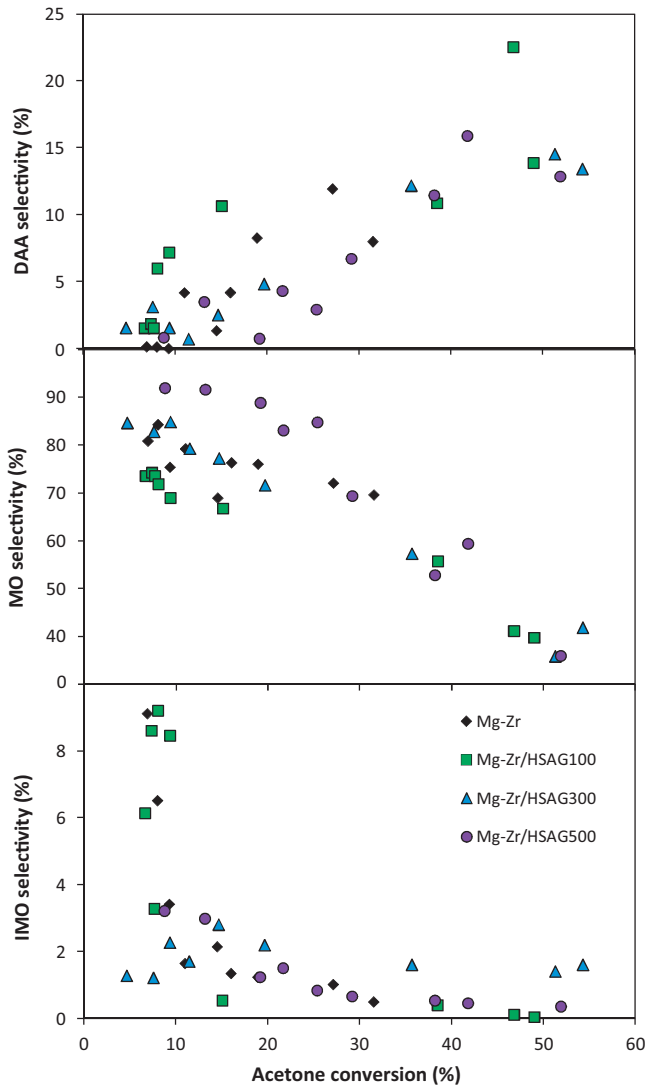

Fig. 7. Evolution of the main C6 products selectivities with the acetone conversion obtained at each temperature with the different catalysts tested.

typical trend of a reactive primary product, showing a continuous decrease of the selectivity with the conversion. In addition, the obtained patterns are very similar for all the catalysts with the only significant difference of the higher selectivities showed by the HSAG500 at lower conversions. This fact seems related to the lower extent of side reactions. By contrast, the behavior of the DAA is completely unexpected, since DAA selectivity shows the same behavior with the three catalysts: increase of the selectivity with conversion, trending to zero selectivity at the lowest conversions. These results suggest that there are two different distributions of active sites in these catalysts that can influence on the products obtained with the acetone condensation: those isolated from any other acid site (therefore not being able to form MO or IMO) and others in the vicinity of acid sites yielding dehydration products. The mechanism of the acetone aldol condensation suggested by these interactions between basic and acid sites is detailed in Scheme 1 and is in good agreement with previous works carried out using isotopic labeling [10] and similar catalysts [25]. Considering that the bulk and HSAG100-supported catalyst present the lowest concentration of weak acid sites and the highest DAA selectivity (Fig. 7), it suggests that these weak acid sites are needed for the DAA dehydration.

At temperatures above 550 K the behavior is different and the formation of trimmers is more relevant. The C9 formation requires

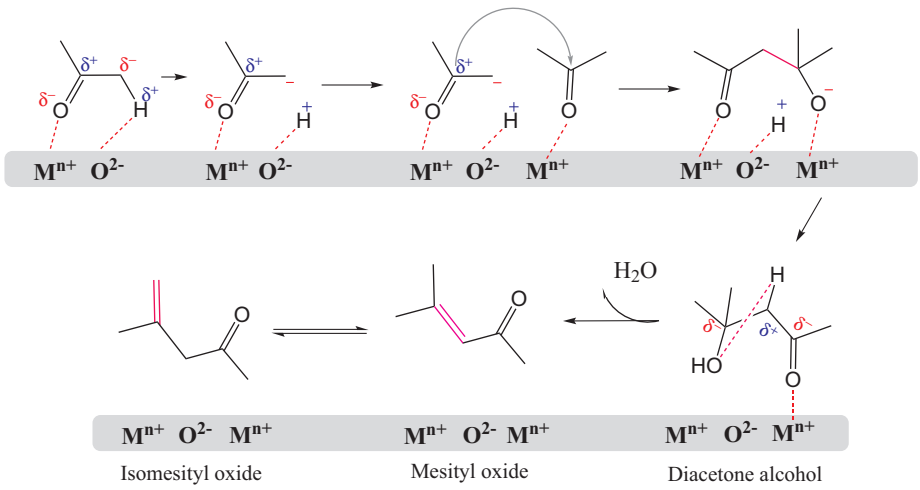

Scheme 1. Reaction mechanism for the acetone self-condensation: diaceton alcohol and mesityl oxide formation.

more temperature and stronger basic sites than the acetone condensation, because the abstraction of the α-proton of mesityl oxide is more difficult (the α-proton of mesityl oxide is less acid than the one of acetone) [5,27].

Concerning to the C6 compounds, the selectivities follow the same order as at lower temperatures. It suggests that the increment in the temperature does not affect the first condensation mechanism, being the most important parameter the relationship between medium-strength basicity and low acidity (acid–base pair of bidentate centers). However, values obtained are considerably lower, mainly in the case of MgZr/HSAG500 (ca. 50%). The high dispersion of the active phase obtained with this support can justify a higher activity for the second condensation, leading to a fast consumption of the C6 compounds. At these temperatures, the selectivity of mesityl oxide decreases because it reacts with acetone yielding C9 trimmers. The above-mentioned increase of DAA selectivity with the acetone conversion, suggests that this compound does not participate in further condensations.

The selectivity evolution of trimmers as function of the acetone conversion is analyzed in Fig. 8. Phorone profiles are congruent with a reactive intermediate that needs the previous formation of other compound (MO) and reacts forming other products (isophorones). On the other hand, isophorones and mesitylene profiles present a continuous increase with the conversion, typical of final products. The only exception is the formation of isophorones over the bulk Mg–Zr oxide, which presents a maximum in the selectivity at intermediate reactant conversion, suggesting that this catalyst is the only which can catalyze isophorone reactions.

The formation of linear trimmer (P) compounds requires the condensation of MO with acetone. Three different peaks were identified in the chromatographic analysis, related to three different phorones. However, their similar molecular weight makes difficult to completely resolve them and they are considered together. The presence of these three isomers implies different interactions between the reactants and the catalytic surface. This fact was previously observed by Salvapati et al. [28], resulting in the mechanisms summarized in Scheme 2. If the MO is adsorbed over the strongest basic sites (monodentate) and the enolate is formed from an acetone adsorbed over a medium-strength basic site, the phorones is obtained by a Michael addition mechanism (2A). This phorone, labeled as P(A), is the majority phorone detected in all the cases (more than 70%), mainly with MgZr/HSAG100, reaching more than 80%. If both mesityl oxide and acetone are adsorbed over medium-strength basic sites, the phorones formation was carried out by aldol condensation. Two different phorones can be obtained by this mechanism, depending on the enolate precursor: acetone (2B) or mesityl oxide (2C). The mechanism 2B requires same basicity strength than the formation of the mesityl oxide, whereas the other two mechanisms need stronger basic sites, due to the lower acidity of the α-proton of mesityl oxide. This explains that the maximum

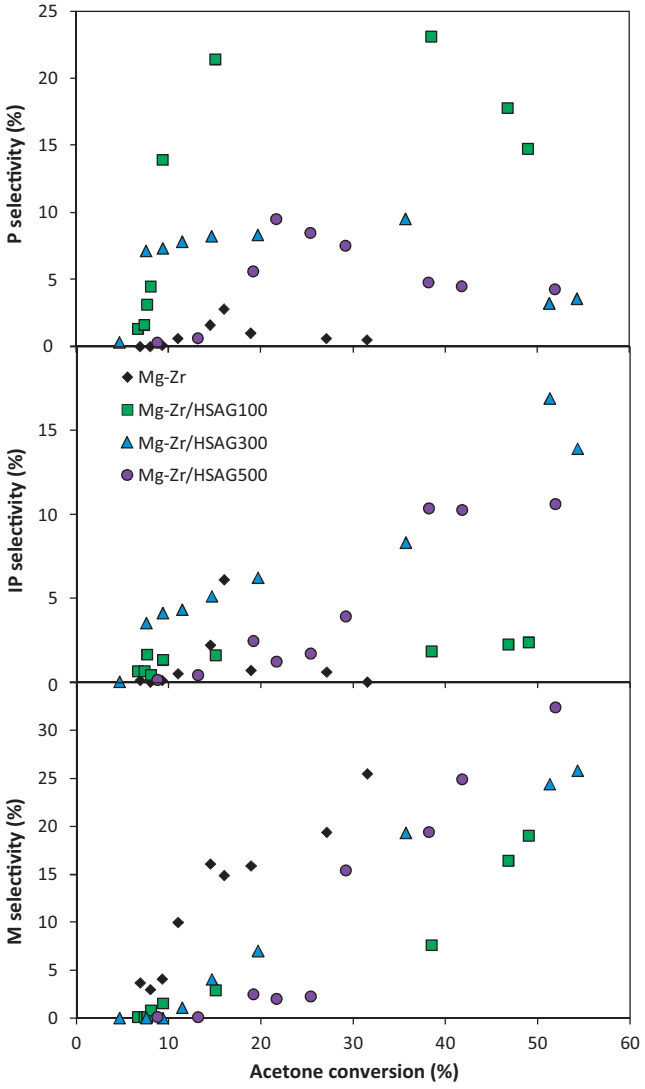

Fig. 8. Evolution of the main C9 products selectivities with the acetone conversion obtained at each temperature with the different catalysts tested.

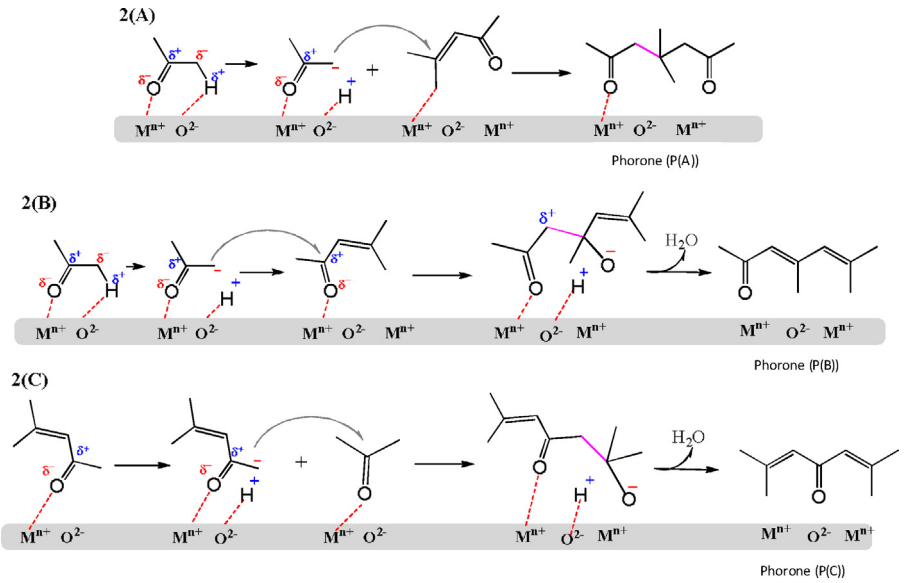

Scheme 2. Reaction mechanism for the second step in the gas-phase acetone self-condensation: linear trimmers formation by Michael addition (2A) or aldol condensation (2B and 2C).

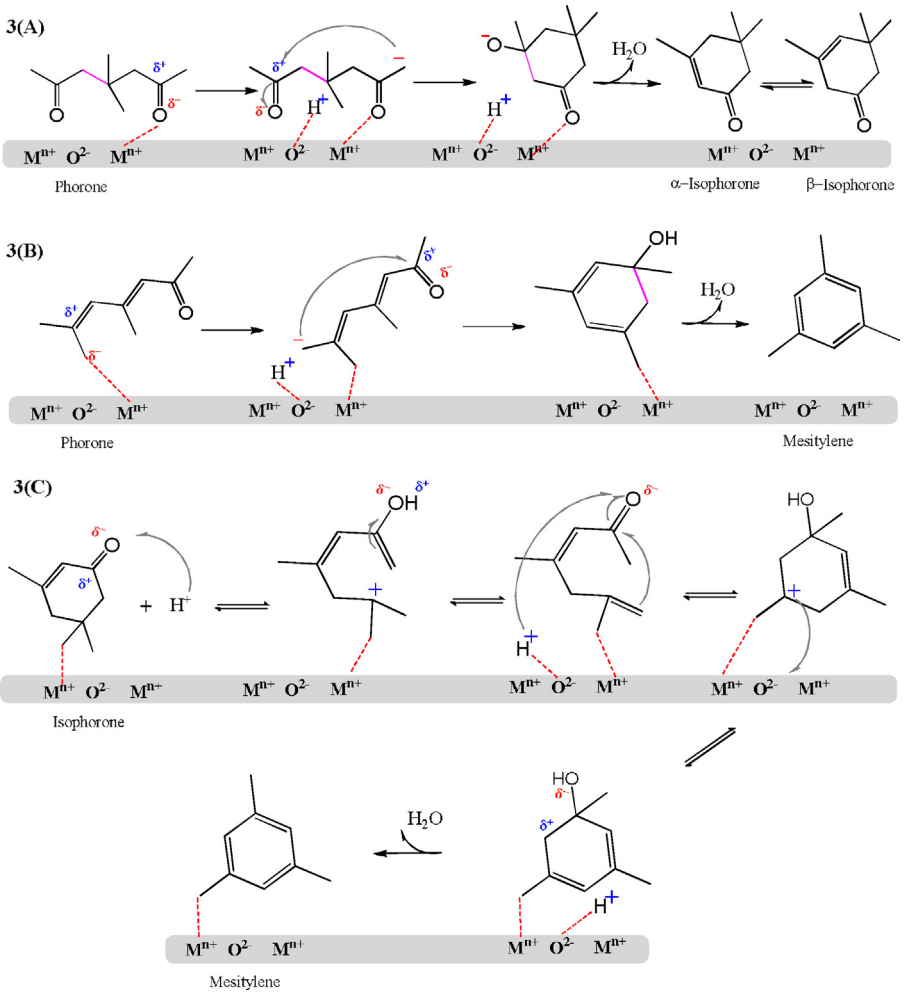

Scheme 3. Reaction mechanism for the third step in the gas-phase acetone self-condensation: cyclations of phorones, obtaining isophorones (3A) and mesitylene (3B). Isophorones rearrangement to mesitylene (3C).

phorone selectivities follows the strongest basic sites concentration order (MgZr/HSAG100 > MgZr/HSAG500 > MgZr/HSAG300). It is also remarkable the low selectivity observed for phorones formation over the bulk catalyst, suggesting that this catalyst catalyze further reactions of this compound.

Concerning to the isophorone (a mixture of α- and β-isomers) which is most valuable C9 compound, only the catalysts supported on HSAG500 and HSAG300, provided significant selectivities for the formation of this compound (up to 15% with HSAG300). In both cases, the observed selectivity pattern corresponds to final products, not undergoing further reactions. In the case of the HSAG100-supported catalysts, very low selectivity (<2%) was obtained in all the studied interval, whereas in the case of the bulk catalyst, selectivity reaches a maximum and decreases at high temperatures, suggesting that this material catalyzes further isophorone transformations. The most evident route for the isophorone formation is the intramolecular aldol condensation of the phorone with two carbonyl groups (A) (isomer formed at highest extent), requiring the presence of strong basic sites (bidentantes and monodentates), as shown in Scheme 3 (reaction 3A). The proposed mechanism is in good agreement with previous studies reported in the literature [29].

However, this desired reaction competes with other side reactions involving the formation of mesitylene. These reactions are undesired since the economic value of this compound is largely lower, and these reactions lead to the formation of aromatic compounds, further condensation of these compounds leading to formation of solid organic deposits. In good agreement with this last fact, HSAG100-supported catalyst bears the lowest amount of carbon deposits and presents the lowest selectivity for mesitylene formation.

The chemistry of the mesitylene formation from lineal phorones is rather complex, involving both base-catalyzed reactions (1,6-Michel addition from phorone (B), according to the mechanism 3(B) shown in Scheme 3) and acid-catalyzed reactions, such as all the de-hydration steps involved. Mesitylene can be also formed from isophorones, but only involving acid sites (mechanism 3C). The formation of mesitylene from isophorones at high temperatures in the presence of acid sites was previously observed in the literature, but with lower selectivities [30,31]. Therefore, the higher mesitylene selectivities observed with the bulk catalysts are in good agreement with isophorone selectivity profile and with the high concentration of medium and strong acid sites (not observed for the supported catalysts), suggesting an important role of the mechanism 3C. By contrast, supported catalysts (HSAG300 and HSAG500) yield mesitylene from phorones, through mechanism 3B. This mechanism needs the presence of both basic and weak acid sites, which are present in these materials. The generation of mesitylene over the HSAG100-supported material follows a different pattern, yielding the lowest selectivities to mesitylene. This fact is explained considering the lower global acidity of this material in comparison to the other catalysts.

5. Conclusions

Bulk Mg–Zr oxides provide good performance for the acetone gas-phase self condensation, obtaining conversions higher than 30% and more than 35% of C9 selectivity. This performance can be improved by supporting the active phase over high surface area graphites (HSAG) using the co-precipitation method, with an increase in the conversion (54.3%) and in the C9 selectivity (49.3%). Other impregnation method and support (nanofibers) were tested with no so promising results. The product distribution obtained depends on the temperature and the acid–basic properties of the catalysts. At low temperature the mesityl oxide selectivity reaches values higher than 85% whereas at high temperatures the presence of trimmers is much more noticeable.

The acidity and basicity distribution of supported materials can be controlled by using HSAG with different surface areas, in such a way that phorones are favored by a high concentration of strong basic sites (MgZr/HSAG100), isophorones need the presence of weak acidity (MgZr/HSAG300) and a good dispersion and balance between basicity and acidity increases the selectivity of mesitylene (MgZr/HSAG500).

Acknowledgements

This work was supported by the Spanish Government (contract CTQ2011-29272-C04-02). L. Faba thanks the Government of the Principality of Asturias for a Ph.D. fellowship (Severo Ochoa Program).

References

[1] S. Sifniades, A.B. Levy, Ullmann's Encyclopedia of Industrial Chemistry, 6th ed., Wiley-VCH, New York, 2002.
[2] N. Qureshi, T. Ezeji, Biofuels Bioproducts and Biorefining 2 (2008) 319.
[3] D. Mansur, T. Yoskikama, K. Norinaga, J. Hayashi, T. Tago, T. Masuda, Fuel 103 (2013) 130.
[4] K. Weisssermel, H.-J. Arpe, Industrial Organic Chemistry, 3rd ed., Wiley, Weinheim, 1997.
[5] M. Paulis, M. Martín, D.B. Soria, A. Díaz, J.A. Odriozola, M. Montes, Applied Catalysis A 180 (1999) 411.
[6] P. Kustrowski, D. Sulkowska, L. Chmielarz, A. Rafalska-Lasocha, B. Dudek, R. Dziembaj, Microporous and Mesoporous Materials 78 (2005) 11.
[7] P.J. Darda, V.V. Ranade, Chemical Engineering Journal 207 (2012) 349.
[8] J.R. Walton, B. Yeomans, Isophorone production using a potassium hydroxide catalyst, US Patent 3,981,918 (1976).
[9] S. Ordóñez, E. Díaz, M. León, L. Faba, Catalysis Today 167 (2011) 71.
[10] M.G. Álvarez, A.M. Frey, J.H. Bitter, A.M. Segarra, K.P. de Jong, F. Medina, Applied Catalysis B 134–135 (2013) 231.
[11] J.I. Di Cosimo, V.K. Díez, C.R. Apesteguía, Applied Catalysis A 137 (1996) 149.
[12] L. Faba, E. Díaz, S. Ordóñez, Applied Catalysis B 113 (2012) 201.
[13] H. Kanai, M. Shono, S. Imamura, H. Kobayashi, Journal of Molecular Catalysis A 130 (1998) 187.
[14] F. Winter, V. Koot, A. Jos van Dillen, J.W. Geus, K.P. de Jong, Journal of Catalysis 236 (2005) 91.
[15] L. Faba, E. Díaz, S. Ordóñez, ChemSusChem 6 (2013) 463.
[16] S. Ordóñez, E. Díaz, R.F. Bueres, E. Asedegbega-Nieto, H. Sastre, Journal of Catalysis 272 (2010) 158.
[17] E. Díaz, S. Ordóñez, R.F. Bueres, E. Asedegbega-Nieto, H. Sastre, Applied Catalysis B 99 (2010) 181–190.
[18] M.A. Aramendía, V. Borau, C. Jiménez, A. Marinas, J.M. Marinas, J.R. Ruiz, F.J. Urbano, Journal of Molecular Catalysis A 218 (2004) 81.
[19] M.R. Cuervo, E. Asedegbega-Nieto, E. Díaz, S. Ordóñez, A. Vega, A.B. Dongil, I. Rodríguez-Ramos, Carbon 46 (2008) 2096.
[20] M. Zamora, T. López, R. Gómez, M. Asomoza, R. Meléndrez, Applied Surface Science 252 (2005) 828.
[21] C.P. Kelkar, A.A. Shultz, Applied Clay Science 13 (1998) 417.
[22] J.I. Di Cosimo, V.K. Díez, M. Xu, E. Iglesia, C.R. Apesteguía, Journal of Catalysis 178 (1998) 499.
[23] W.K. O'Keefe, M. Jiang, F.T.T. Ng, G.L. Rempel, Chemical Engineering Science 60 (2005) 4131.
[24] G.G. Podrebarac, F.T.T. Ng, G.L. Rempel, Chemical Engineering Science 52 (1997) 2991.
[25] V.K. Díez, C.R. Apesteguía, J.I. DiCosimo, Journal of Catalysis 240 (2006) 235.
[26] G.D. Yadav, P. Aduri, Journal of Molecular Catalysis A 355 (2012) 142.
[27] A.A. Nikolopoulos, B.W.L. Jang, J.J. Spivey, Applied Catalysis A 296 (2005) 128.
[28] G.S. Salvapati, K.V. Ramanamurty, M. Janardanarao, Journal of Molecular Catalysis 54 (1989) 9.
[29] D.S. Torok, W.J. Scott, Tetrahedron Letters 34 (1993) 3067.
[30] M. Zamora, T. López, M. Asomoza, R. Meléndrez, R. Gómez, Catalysis Today 116 (2006) 234.
[31] V. Siva Kumar, B.M. Nagaraja, V. Shashikala, P. Seetharamulu, A.H. Padmasri, B. David Raju, K.S. Rama Rao, Journal of Molecular Catalysis A 223 (2004) 283.